Spatial multipartite entanglement and localization of entanglement

D. Daems and N. J. Cerf
QuIC, Ecole Polytechnique, Université Libre de Bruxelles, B-1050 Brussels, Belgium
(Received 13 October 2009; published 9 September 2010)

We present a simple model together with its physical implementation which allows one to generate multipartite entanglement between several spatial modes of the electromagnetic field. It is based on parametric down-conversion with N pairs of symmetrically tilted plane waves serving as a pump. The characteristics of this spatial entanglement are investigated in the cases of zero as well as nonzero phase mismatch. Furthermore, the phenomenon of entanglement localization in just two spatial modes is studied in detail and shown to result in an enhancement of the entanglement by a factor $\sqrt{N}$.

DOI: 10.1103/PhysRevA.82.032303 PACS number(s): 03.67.Bg, 42.65.Lm

I. INTRODUCTION

The existence of entanglement between more than two parties for discrete or continuous quantum variables is one of the most striking predictions of quantum mechanics. At the fundamental level, characterizing multipartite entanglement has raised much interest since the pioneering work of Coffman *et al.* [1] for qubit systems. The case of continuous-variable multimode Gaussian states has been addressed by Adesso *et al.* [2–5]. The interest in multipartite entanglement is motivated not only by fundamental questions, but also by its potential for applications in quantum communication technologies. Possible applications of continuous-variable (CV) multipartite entanglement include quantum teleportation networks, quantum telecloning, controlled quantum dense coding, and quantum secret sharing (see Ref. [6] and references therein).

A number of schemes to generate CV multipartite entanglement have been proposed theoretically and realized experimentally in recent years. There were first the passive optical scheme using squeezed states mixed with beam splitters [7]. Squeezing using cascaded nonlinearity was observed experimentally by Kasai *et al.* [8]. Then came the active schemes in which multipartite entanglement is created as a result of parametric interaction of several optical waves such as cascaded or concurrent [9–11], interlinked [12,13], or consecutive parametric interactions [14]. These schemes generally neglect the spatial structure of the electromagnetic field, which is of importance. Transverse momenta are another way of defining an image, and the quantum properties of parametric down-converted images have been extensively investigated (see Refs. [15,16] and references therein).

It is natural to investigate whether the spatial modes can also serve for the creation of CV multipartite entanglement. Entangling the spatial properties of laser beams has been achieved by Wagner *et al.* [17]. The multimode quantum properties of a perfectly spatially degenerate (self-imaging) optical parametric oscillator have been studied by Lopez *et al.* [18]. A beautiful experiment applying spatial degrees of freedom, although not by structuring the pump as in quantum images, to quantum key distribution is described in Ref. [19]. The generation of entanglement among three bright beams of light of different wavelengths has also been demonstrated [20]. A simple active scheme for the creation of tripartite entanglement between spatial modes of the electromagnetic field has been proposed in Ref. [21]. It consists in pumping a nonlinear parametric medium by a coherent combination of several tilted plane monochromatic waves which is called a spatially structured pump. Since the pump photons can be extracted from any of these waves and the pair of down-converted photons can be emitted in different directions according to the phase-matching condition, that scheme allows for the creation of tripartite entanglement between spatial modes of the down-converted field.

The aim of this paper is to generalize the results of Ref. [21] to the generation of spatial multipartite entanglement. For that purpose, we present a scheme with an arbitrary number $2N$ of tilted plane waves pumping a parametric medium. An interesting feature of this realistic proposal is the possibility of localizing the created spatial multipartite entanglement in just two well-defined spatial modes formed as a linear combination of all the modes participating in the down-conversion process. The possibility of entanglement localization was introduced by Serafini *et al.* [3] and a physical implementation was also given in terms of $2N-1$ beam splitters and $2N$ single-mode squeezed inputs based on Ref. [22]. The localization of entanglement is also considered, in a different context, in Ref. [23]. The paper is organized as follows. Section II is devoted to spatial multipartite entanglement. We present the process of parametric down-conversion with a spatially structured pump consisting of N pairs of symmetrically tilted plane waves in Sec. II A. The evolution equations for the field operators are given and solved in the rotating wave approximation for possibly nonzero constant phase mismatch. The inseparability property of the generated state is then studied In Sec. II B. Section III is dedicated to the phenomenon of entanglement localization. It is presented explicitly in Sec. III A and a quantitative characterization of the spatial entanglement generated by this process is given in Sec. III B. The scaling with N as well as the dependence on the phase mismatch are explicitly provided. Conclusions are drawn in Sec. IV.

II. SPATIAL MULTIPARTITE ENTANGLEMENT

A. Parametric down-conversion with spatially structured pump

We consider a system of pumps which consists of N pairs of symmetrically tilted plane waves

$$E_p(\mathbf{r}) = \frac{\alpha}{4\pi^2}\sum_{d=1}^{N}(e^{i\mathbf{q}_d\cdot\mathbf{r}} + e^{-i\mathbf{q}_d\cdot\mathbf{r}}), \tag{1}$$

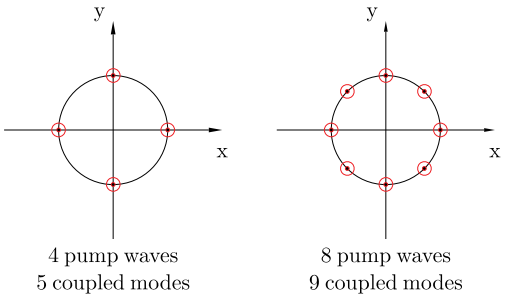

FIG. 1. (Color online) Scheme for the generation of spatial multipartite entanglement with $2N$ symmetrically tilted pump waves (illustrated for $N=2$ and 4). The little circles represent the projections of the pump wave vectors in the xy plane of the crystal entering face.

with $\mathbf{r}=(x,y)$, the vector of coordinates in the plane of the crystal entering face, and $\mathbf{q}=(k_x,k_y)$, the projection of the three-dimensional wave vector $\mathbf{k}$ in that plane. Its Fourier transform in the xy plane of the (infinite) crystal (entering face) corresponds to Dirac delta's centered in $\mathbf{q_d}$ and $-\mathbf{q_d}$

$$E_p(\mathbf{q})=\alpha\sum_{d=1}^{N}[\delta(\mathbf{q}-\mathbf{q}_d)+\delta(\mathbf{q}+\mathbf{q}_d)]\,. \tag{2}$$

This scheme is illustrated in Fig. 1 for $N=2$ and 4. The little circles represent the projections of the pump wave vectors in the xy plane of the crystal entering face. The plane depicted in Fig. 2 is the one going through one of the N pairs of opposed pumps on Fig. 1, for example the yz plane.

The evolution of the annihilation and creation operators $\hat{a}$ and $\hat{a}^\dagger$ associated to the propagation and diffraction of the quantized electromagnetic field through the nonlinear parametric medium is described by [24]

$$\frac{\partial}{\partial z}\hat{a}(z,\mathbf{q})=\lambda\int\mathbf{dq}'E_p(\mathbf{q}-\mathbf{q}')\hat{a}^\dagger(z,-\mathbf{q}')e^{i\Delta(\mathbf{q},-\mathbf{q}')z}. \tag{3}$$

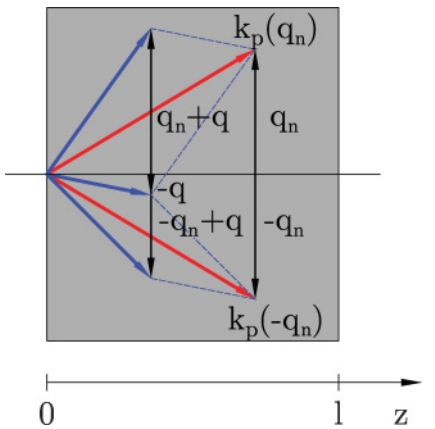

FIG. 2. (Color online) The plane depicted is the one passing through one of the N pairs of opposed pumps on Fig. 1 (e.g., the yz plane). The tilted pumps have wave vectors $\mathbf{k}_p(\pm\mathbf{q}_n)$ with n ranging from 1 to N. The transverse (vertical) components of these wave vectors are denoted $\pm\mathbf{q}_n$ [see below (1) for a definition].

Here z is the longitudinal coordinate and Δ is the phase mismatch defined as

$$\Delta(\mathbf{q},-\mathbf{q}')=k_z(\mathbf{q})+k_z(-\mathbf{q}')-k_{pz}(\mathbf{q}-\mathbf{q}'), \tag{4}$$

where $k_z(q)$ and $k_z(-q)$ are the longitudinal components of the two incoming wave vectors and k_{pz} is the longitudinal component of the pump wave vector. The conservation of energy and momentum imply that we have to consider a set of $2N+1$ coupled equations, obtained upon substitution of (2) into (3), for the waves exiting the crystal with wave vector transverse components $\mathbf{q}$, $\mathbf{q}_j-\mathbf{q}$, and $-\mathbf{q}_j-\mathbf{q}$ with $j=1,\ldots,N$:

$$\begin{aligned}\frac{\partial}{\partial z}\hat{a}(z,\mathbf{q})&=\alpha\lambda\sum_{d=1}^{N}\{\hat{a}^\dagger(z,\mathbf{q}_d-\mathbf{q})e^{i\Delta(\mathbf{q},\mathbf{q}_d-\mathbf{q})z}\\&\quad+\hat{a}^\dagger(z,-\mathbf{q}_d-\mathbf{q})e^{i\Delta(\mathbf{q},-\mathbf{q}_d-\mathbf{q})z}\},\\\frac{\partial}{\partial z}\hat{a}(z,\pm\mathbf{q}_j+\mathbf{q})&\\&=\alpha\lambda\sum_{d=1}^{N}\{\hat{a}^\dagger(z,\mathbf{q}_d\mp\mathbf{q}_j-\mathbf{q})e^{i\Delta(\mathbf{q},\mathbf{q}_d\mp\mathbf{q}_j-\mathbf{q})z}\\&\quad+\hat{a}^\dagger(z,-\mathbf{q}_d\mp\mathbf{q}_j-\mathbf{q})e^{i\Delta(\mathbf{q},-\mathbf{q}_d\mp\mathbf{q}_j-\mathbf{q})z}\}.\end{aligned} \tag{5}$$

In the second equation, the phase mismatch is higher for the contributions with $d\neq j$, which shall therefore be neglected. This corresponds to the usual rotating wave approximation. The other phase mismatches are all taken equal to Δ, which amounts to imposing some symmetries on $\Delta(\pm\mathbf{q},\pm\mathbf{q}_d\pm\mathbf{q})$. One may introduce a renormalized phase mismatch δ and a new relevant variable $\tilde{r}$ which combines the interaction strength $\alpha\lambda$ and the longitudinal coordinate z

$$\begin{aligned}\delta&\equiv\frac{\Delta}{2\sqrt{2}\alpha\lambda},\\\tilde{r}&\equiv\sqrt{2}\alpha\lambda z.\end{aligned} \tag{6}$$

We shall use the following notation:

$$\begin{aligned}a_0(\tilde{r})&\equiv\hat{a}(z,\mathbf{q}),\\a_{n_\pm}(\tilde{r})&\equiv\hat{a}(z,\pm\mathbf{q}_n+\mathbf{q}),\quad n=1,\ldots,N,\end{aligned} \tag{7}$$

and shall consider only the zeroth spatial Fourier components of the field $\mathbf{q}=\mathbf{0}$. Physically, this corresponds to photodetection of the light field by a single large photodetector without spatial resolution. These modes are depicted in Fig. 2: the long (blue) arrows pertain to $\hat{a}_{n_\pm}(0)$, the short ones to $\hat{a}_0^\dagger(0)$. Strictly speaking, these modes represent a continuum of modes and cannot be treated in a general situation as plane waves. However, here we shall make the approximation of discrete plane waves. A discussion on the precision to which the wave vectors are defined can be found in Ref. [18]. In this setting, one can then rewrite (5) as

$$\begin{aligned}\frac{d}{d\tilde{r}}\hat{a}_0&=\frac{e^{2i\delta\tilde{r}}}{\sqrt{2}}\sum_{d=1}^{N}(\hat{a}_{d_+}^\dagger+\hat{a}_{d_-}^\dagger),\\\frac{d}{d\tilde{r}}\hat{a}_{n_\pm}&=\frac{e^{2i\delta\tilde{r}}}{\sqrt{2}}\hat{a}_0^\dagger,\quad n=1,\ldots,N.\end{aligned} \tag{8}$$

We may solve this set of equations and obtain for the fields at the output of the crystal, $r = \tilde{r}|_{z=\ell}$,

$$\begin{aligned}\hat{a}_0(r) &= U(r)\hat{a}_0(0) + \frac{V(r)}{\sqrt{2N}}\sum_{d=1}^{N}\{\hat{a}^\dagger_{d_+}(0) + \hat{a}^\dagger_{d_-}(0)\},\\ \hat{a}_{n_\pm}(r) &= \hat{a}_{n_\pm}(0) + \frac{U(r)-1}{\sqrt{2N}}\sum_{d=1}^{N}\{\hat{a}_{d_+}(0) + \hat{a}_{d_-}(0)\}\\ &\quad + \frac{V(r)}{\sqrt{2N}}\hat{a}^\dagger_0(0), \quad n = 1,\ldots,N.\end{aligned} \tag{9}$$

The functions $U(r)$ and $V(r)$, which satisfy $|U(r)|^2 - |V(r)|^2 = 1$, are given by

$$\begin{aligned}U(r) &= e^{i\delta r}\left(\cosh(\sqrt{N}\gamma r) - i\frac{\delta}{\sqrt{N}\gamma}\sinh(\sqrt{N}\gamma r)\right)\\ V(r) &= e^{i\delta r}\frac{1}{\gamma}\sinh(\sqrt{N}\gamma r),\end{aligned} \tag{10}$$

where γ depends on the reduced phase mismatch δ,

$$\gamma = \sqrt{1 - \frac{\delta^2}{N}}. \tag{11}$$

In the next section we shall characterize these solutions for the fields at the output of the crystal.

B. Multipartite entanglement

The parametric down-conversion process preserves the Gaussian character of incoming modes. Hence the outgoing modes are Gaussian states which are thus completely characterized by the covariance matrix associated with their quadrature components

$$\begin{aligned}\hat{x}_0(r) &\equiv 2\mathrm{Re}\,\hat{a}_0(r),\\ \hat{p}_0(r) &\equiv 2\mathrm{Im}\,\hat{a}_0(r),\\ \hat{x}_{n_\pm}(r) &\equiv 2\mathrm{Re}\,\hat{a}_{n_\pm}(r),\\ \hat{p}_{n_\pm}(r) &\equiv 2\mathrm{Im}\,\hat{a}_{n_\pm}(r), \quad n = 1,\ldots,N.\end{aligned} \tag{12}$$

From the solution (9) one obtains

$$\begin{aligned}\hat{x}_0(r) &= \mathrm{Re}\,U(r)\hat{x}_0(0) - \mathrm{Im}\,U(r)\hat{p}_0(0) + \sum_{d=1}^{N}\left\{\mathrm{Re}\,V(r)\frac{\hat{x}_{d_+}(0)+\hat{x}_{d_-}(0)}{\sqrt{2N}} + \mathrm{Im}\,V(r)\frac{\hat{p}_{d_+}(0)+\hat{p}_{d_-}(0)}{\sqrt{2N}}\right\},\\ \hat{p}_0(r) &= \mathrm{Im}\,U(r)\hat{x}_0(0) + \mathrm{Re}\,U(r)\hat{p}_0(0) + \sum_{d=1}^{N}\left\{\mathrm{Im}\,V(r)\frac{\hat{x}_{d_+}(0)+\hat{x}_{d_-}(0)}{\sqrt{2N}} - \mathrm{Re}\,V(r)\frac{\hat{p}_{d_+}(0)+\hat{p}_{d_-}(0)}{\sqrt{2N}}\right\},\\ \hat{x}_{n_\pm}(r) &= \frac{\mathrm{Re}\,V(r)}{\sqrt{2N}}\hat{x}_0(0) + \frac{\mathrm{Im}\,V(r)}{\sqrt{2N}}\hat{p}_0(0) + \hat{x}_{n_\pm}(0) + \sum_{d=1}^{N}\left\{(\mathrm{Re}\,U(r)-1)\frac{\hat{x}_{d_+}(0)+\hat{x}_{d_-}(0)}{2N} - \mathrm{Im}\,U(r)\frac{\hat{p}_{d_+}(0)+\hat{p}_{d_-}(0)}{2N}\right\},\\ \hat{p}_{n_\pm}(r) &= \frac{\mathrm{Im}\,V(r)}{\sqrt{2N}}\hat{x}_0(0) - \frac{\mathrm{Re}\,V(r)}{\sqrt{2N}}\hat{p}_0(0) + \hat{p}_{n_\pm}(0) + \sum_{d=1}^{N}\left\{\mathrm{Im}\,U(r)\frac{\hat{x}_{d_+}(0)+\hat{x}_{d_-}(0)}{2N} + (\mathrm{Re}\,U(r)-1)\frac{\hat{p}_{d_+}(0)+\hat{p}_{d_-}(0)}{2N}\right\}.\end{aligned} \tag{13}$$

We can now determine the covariance matrix elements $\sigma_{ij} \equiv \langle(\Delta\hat{\xi}_i\Delta\hat{\xi}_j + \Delta\hat{\xi}_j\Delta\hat{\xi}_i)/2\rangle$ of the output state ρ with $\langle\cdot\rangle \equiv \mathrm{Tr}(\rho\,\cdot)$ and $\Delta\hat{\xi}_i \equiv \hat{\xi}_i - \langle\hat{\xi}_i\rangle$ where $\hat{\xi}_i$ is some component of the vector $\hat{\xi} = (\hat{x}_0,\hat{p}_0,\hat{x}_{1_+},\hat{p}_{1_+},\hat{x}_{1_-},\hat{p}_{1_-},\hat{x}_{2_+},\hat{p}_{2_+},\ldots,\hat{x}_{N_-},\hat{p}_{N_-})$. Taking into account that all inputs are vacuum states we obtain from (13)

$$\begin{aligned}\langle[\hat{x}_0(r)]^2\rangle &= \langle[\hat{p}_0(r)]^2\rangle = a,\\ \langle[\hat{x}_{n_\pm}(r)]^2\rangle &= \langle[\hat{p}_{n_\pm}(r)]^2\rangle = 1 + \frac{a-1}{2N},\\ \langle\hat{x}_{n_\pm}(r)\hat{x}_{d_\pm}(r)\rangle &= \langle\hat{x}_{n_\pm}(r)\hat{x}_{d_\mp}(r)\rangle = \frac{a-1}{2N},\\ \langle\hat{p}_{n_\pm}(r)\hat{p}_{d_\pm}(r)\rangle &= \langle\hat{p}_{n_\pm}(r)\hat{p}_{d_\mp}(r)\rangle = \frac{a-1}{2N},\\ \langle\hat{x}_0(r)\hat{x}_{n_\pm}(r)\rangle &= -\langle\hat{p}_0(r)\hat{p}_{n_\pm}(r)\rangle = \frac{b}{\sqrt{2N}},\\ \langle\hat{x}_0(r)\hat{p}_{n_\pm}(r)\rangle &= \langle\hat{p}_0(r)\hat{x}_{n_\pm}(r)\rangle = \frac{c}{\sqrt{2N}},\\ \langle\hat{x}_0(r)\hat{p}_0(r)\rangle &= \langle\hat{x}_{n_\pm}(r)\hat{p}_{d_\pm}(r)\rangle = \langle\hat{x}_{n_\pm}(r)\hat{p}_{d_\mp}(r)\rangle = 0,\end{aligned} \tag{14}$$

for $n,d = 1,\ldots,N$, with

$$\begin{aligned}a &\equiv |U|^2 + |V|^2,\\ b &\equiv 2(\mathrm{Re}\,U\ \mathrm{Re}\,V - \mathrm{Im}\,U\ \mathrm{Im}\,V),\\ c &\equiv 2(\mathrm{Re}\,U\ \mathrm{Im}\,V + \mathrm{Im}\,U\mathrm{Re}\,V).\end{aligned} \tag{15}$$

Ordering the lines and columns according to $\hat{x}_0,\hat{p}_0,\hat{x}_{1_+},\hat{p}_{1_+},\hat{x}_{1_-},\hat{p}_{1_-},\hat{x}_{2_+},\hat{p}_{2_+},\ldots,\hat{x}_{N_-},\hat{p}_{N_-}$, the covariance matrix reads then

$$\sigma = \begin{pmatrix} A & D & D & D & \cdots & D & D & D\\ D & B & C & C & \cdots & C & C & C\\ D & C & B & C & \cdots & C & C & C\\ D & C & C & B & \cdots & C & C & C\\ \vdots & \vdots & \vdots & \vdots & \ddots & \vdots & \vdots & \vdots\\ D & C & C & C & \cdots & B & C & C\\ D & C & C & C & \cdots & C & B & C\\ D & C & C & C & \cdots & C & C & B \end{pmatrix}, \tag{16}$$

where A, B, C, and D are the following 2×2 matrices:

$$A = aI_2, \quad B = 1 + \frac{a-1}{2N} I_2, \quad C = \frac{a-1}{2N} I_2,$$
$$D = \frac{1}{\sqrt{2N}} \begin{pmatrix} b & c \\ c & -b \end{pmatrix}, \quad I_2 = \begin{pmatrix} 1 & 0 \\ 0 & 1 \end{pmatrix}. \tag{17}$$

Its symplectic eigenvalues $\{\nu_i\}$ are $\sqrt{a^2 - b^2 - c^2}$ (with a fourfold degeneracy) and 1 (with a $2N-3$ degeneracy). Noting that $b^2 + c^2 = 4|U|^2|V|^2$ implies that $\sqrt{a^2 - b^2 - c^2} = 1$. The product of symplectic eigenvalues is thus unity and as expected for a unitary evolution, the output state remains pure.

The covariance matrix (16) is bisymmetric [i.e., it is invariant under the permutation of quadratures $\hat{x}_{n_\pm}(r), \hat{p}_{n_\pm}(r) \leftrightarrow \hat{x}_{d_\pm}(r), \hat{p}_{d_\pm}(\ell)$ or $\hat{x}_{d_\mp}(r), \hat{p}_{d_\mp}(\ell)$]. As a consequence, it has the multipartite entanglement structure of covariance matrices associated to bisymmetric $(1+2N)$-mode Gaussian states considered in Ref. [3]. We now show that the output state obtained here exhibits multipartite entanglement in the sense of Ref. [22] (i.e., is fully inseparable). For that purpose, we have to verify that the following condition on covariance matrix elements is violated

$$Q \equiv \left\langle \left(\hat{x}_0(r) - \frac{1}{\sqrt{2N}} \sum_{n=1}^{N} \{\hat{x}_{n_+}(r) + \hat{x}_{n_-}(r)\} \right)^2 \right\rangle + \left\langle \left(\hat{p}_0(r) + \frac{1}{\sqrt{2N}} \sum_{n=1}^{N} \{\hat{p}_{n_+}(r) + \hat{p}_{n_-}(r)\} \right)^2 \right\rangle \geqslant \frac{1}{2N}. \tag{18}$$

From (14) and (15) one deduces that

$$\begin{aligned} Q &= 4(a-b) \\ &= 4\{[\mathrm{Re}\, U(r) - \mathrm{Re}\, V(r)]^2 + [\mathrm{Im}\, U(r) + \mathrm{Im}\, V(r)]^2\}. \end{aligned} \tag{19}$$

When the phase matching condition is satisfied $\delta = 0$, one deduces from (10) that $U(r) = \cosh\sqrt{N}r$ and $V(r) = \sinh\sqrt{N}r$. It follows that (19) reduces to

$$Q = 4[\cosh(\sqrt{N}r) - \sinh(\sqrt{N}r)]^2 = 4e^{-2\sqrt{N}r}. \tag{20}$$

This quantity is smaller than $1/2N$ if the squeezing parameter r satisfies

$$r = \sqrt{2}\alpha\lambda\ell > \frac{\ln(8N)}{2\sqrt{N}}. \tag{21}$$

Under this condition on the pump amplitude α, the coupling parameter λ, and the crystal length ℓ, the output state ρ produced by the above parametric down-conversion process with $2N$ symmetrically tilted plane waves therefore exhibits multipartite entanglement. This generalizes the result obtained in Ref. [21] in the case of tripartite entanglement $(N = 1)$.

For a small nonzero phase mismatch, we can expand (19) around $\delta = 0$, which yields

$$Q = 4e^{-2\sqrt{N}r} + \frac{\delta^2}{N}[(3 - 4Nr^2)e^{-2\sqrt{N}r} + 4(2\sqrt{N}r - 1) + (2\sqrt{N}r - 1)^2 e^{2\sqrt{N}r}] + O(\delta^4). \tag{22}$$

Owing to the last term, this quantity increases exponentially with $\sqrt{N}r$. As a consequence, Q remains smaller than $1/2N$ only for low values of the phase mismatch. This suggests that the multipartite entanglement, at least when it is estimated with the criterion (18) is very sensitive to δ. This situation is in contrast with the phenomenon that we study in the next section, namely the localization of entanglement, which will be shown to be robust with respect to the phase mismatch. It probably indicates that (18) is not appropriate to witness all the entanglement existing in the previously generated state since this criterion is simply sufficient but not necessary.

III. LOCALIZATION OF ENTANGLEMENT

A. Beam splitting the output state

It has been shown [3] that the entanglement of bisymmetric $(m+n)$-mode Gaussian states is unitarily *localizable* (i.e., that through local unitary operations it may be fully concentrated in a single pair of modes). We shall study explicitly this phenomenon here. For that purpose we shall perform the following unitary transformation based on discrete Fourier series

$$\begin{aligned} \hat{a}'_0(\tilde{r}) &= \hat{a}_0(\tilde{r}), \\ \hat{a}'_k(\tilde{r}) &= \frac{1}{\sqrt{N}} \sum_{n=1}^{N} \frac{\hat{a}_{n_+}(\tilde{r}) - e^{-\pi i k} \hat{a}_{n_-}(\tilde{r})}{\sqrt{2}} e^{-\pi i (k-1)\frac{n-1}{N}}, \\ & \qquad k = 1, \ldots, 2N. \end{aligned} \tag{23}$$

Physically, this corresponds to beam splitting the quantized fields at the output of the crystal. Indeed, it has been shown [25] that any unitary matrix can be implemented as an optical multiport by a triangular array of beam splitters. Notice that the fraction on the second line of (23) corresponds to the output of a balanced beam splitter. The summation over n then corresponds to the action of an $N \times N$ unitary matrix which can be implemented by $\binom{N}{2} = \frac{N(N-1)}{2}$ appropriate beam splitters acting on every pair of modes [25]. Hence the transformation (23) requires N balanced beam splitters and $N(N-1)$ specific ones, that is, a total of N^2 beam splitters. For example, for $N = 3$, in addition to the three balanced beam splitters, there is another set of four beam splitters with transmittance $1/2$ (one of them with a phase equal to π) and two with transmittance $1/3$.

As a consequence of (23), one deduces from (9) that the new fields at the output of the crystal are transformed to the following ones:

$$\begin{aligned} \hat{a}'_0(r) &= U(r)\hat{a}'_0(0) + V(r)\hat{a}'^{\dagger}_1(0), \\ \hat{a}'_1(r) &= U(r)\hat{a}'_1(0) + V(r)\hat{a}'^{\dagger}_0(0), \\ \hat{a}'_k(r) &= \hat{a}'_k(0), \quad k = 2, \ldots, 2N, \end{aligned} \tag{24}$$

Accordingly, the quadratures are now given by

$$\begin{aligned} \hat{x}'_0(r) &= \mathrm{Re}\, U(r)\hat{x}'_0(0) - \mathrm{Im}\, U(r)\hat{p}'_0(0) \\ &\quad + \mathrm{Re}\, V(r)\hat{x}'_1(0) + \mathrm{Im}\, V(r)\hat{p}'_1(0), \\ \hat{p}'_0(r) &= \mathrm{Re}\, U(r)\hat{p}'_0(0) + \mathrm{Im}\, U(r)\hat{x}'_0(0) \\ &\quad - \mathrm{Re}\, V(r)\hat{p}'_1(0) + \mathrm{Im}\, V(r)\hat{x}'_1(0), \end{aligned}$$

$$\begin{aligned}\hat{x}_1'(r) &= \mathrm{Re}\,U(r)\hat{x}_1'(0) - \mathrm{Im}\,U(r)\hat{p}_1'(0) \\ &\quad + \mathrm{Re}\,V(r)\hat{x}_0'(0) + \mathrm{Im}\,V(r)\hat{p}_0'(0), \\ \hat{p}_1'(r) &= \mathrm{Re}\,U(r)\hat{p}_1'(0) + \mathrm{Im}\,U(r)\hat{x}_1'(0) \\ &\quad - \mathrm{Re}\,V(r)\hat{p}_0'(0) + \mathrm{Im}\,V(r)\hat{x}_0'(0), \\ \hat{x}_k'(r) &= \hat{x}_k'(0), \\ \hat{p}_k'(r) &= \hat{p}_k'(0), \quad k = 2,\ldots,2N. \end{aligned} \tag{25}$$

Hence the covariance matrix elements associated to the density matrix ρ' are

$$\begin{aligned} \langle[\hat{x}_0'(r)]^2\rangle = \langle[\hat{p}_0'(r)]^2\rangle = \langle[\hat{x}_1'(r)]^2\rangle = \langle[\hat{p}_1'(r)]^2\rangle = a, \\ \langle\hat{x}_0'(r)\hat{x}_1'(r)\rangle = -\langle\hat{p}_0'(r)\hat{p}_1'(r)\rangle = b, \\ \langle\hat{x}_0'(r)\hat{p}_1'(r)\rangle = \langle\hat{p}_0'(r)\hat{x}_1'(r)\rangle = c, \\ \langle[\hat{x}_k'(r)]^2\rangle = \langle[\hat{p}_k'(r)]^2\rangle = 1, \quad k = 2,\ldots,2N, \end{aligned} \tag{26}$$

and the other ones are zero. Ordering the lines and columns according to $\hat{x}_0', \hat{p}_0', \hat{x}_1', \hat{p}_1', \hat{x}_2', \hat{p}_2', \ldots, \hat{x}_{2N}', \hat{p}_{2N}'$, the covariance matrix reads

$$\sigma' = \begin{pmatrix} a & 0 & b & c \\ 0 & a & c & -b \\ b & c & a & 0 \\ c & -b & 0 & a \end{pmatrix} \bigoplus I_{2(2N-1)}, \tag{27}$$

where I_k is the $k \times k$ unity matrix. Its symplectic eigenvalues $\{\nu_i'\}$ are the same as those of σ as σ' is obtained by congruence

$$\sigma' = S^{\mathrm{T}}\sigma S, \tag{28}$$

where the elements of the symplectic transformation S are given by (23). In the next section, we investigate the nonseparability properties of the pertaining state ρ'.

B. Logarithmic negativity

The covariance matrix (27) is bisymmetric (i.e., the local exchange of any pairs of modes within its two diagonal blocks leaves the matrix invariant [3]). Notice that here the unitary transformation (23) is such that the covariant matrix σ' is block-diagonal and invariant under the exchange of modes 0 and 1.

The separability of the state ρ' can be determined as in Ref. [3] by (i) considering a partition of the system in two subsystems and (ii) investigating the positivity of the partially transposed matrix $\tilde{\rho}'$ obtained upon transposing the variables of only one of the two subsystems. The positivity of partial transposition (PPT) is a necessary condition for the separability of any bipartite quantum state [26,27]. It is also sufficient for the separability of $(1+n)$-mode Gaussian states [28,29]. The covariance matrix $\tilde{\sigma}'$ of the partially transposed state $\tilde{\rho}'$ with respect to one subsystem is obtained [28] by changing the signs of the quadratures p_j' belonging to that subsystem.

Here because of the block-diagonal structure of σ', we can restrict the analysis to the first block and consider the transposition of mode 1 (i.e., change the sign of p_1')

$$\tilde{\sigma}' = \begin{pmatrix} a & 0 & b & c \\ 0 & a & -c & b \\ b & -c & a & 0 \\ c & b & 0 & a \end{pmatrix} \bigoplus I_{2(2N-1)}. \tag{29}$$

Its symplectic eigenvalues $\{\tilde{\nu}_j'\}$ are 1 and

$$\tilde{\nu}_\pm' \equiv a \pm \sqrt{b^2 + c^2} = (|U| \pm |V|)^2. \tag{30}$$

The necessary and sufficient PPT condition for the separability of the state ρ' amounts to having $\tilde{\nu}_j' \geqslant 1 \forall j$. We can therefore focus on the smallest eigenvalue $\tilde{\nu}_-'$. The extent to which this criterion is violated is measured by $\mathcal{E}_{\mathcal{N}}(\rho')$, the logarithmic negativity of ρ' defined as the logarithm of the trace norm of $\tilde{\rho}'$

$$\mathcal{E}_{\mathcal{N}}(\rho') = \ln ||\tilde{\rho}'||_1 = \max(0, -\ln \tilde{\nu}_-'), \tag{31}$$

where $\tilde{\nu}_-'$ is obtained explicitly from (30) and (10) as

$$\begin{aligned} \tilde{\nu}_-' = \frac{1}{\gamma^2}\Bigg(\sqrt{1 - \frac{\delta^2}{N\cosh^2(\sqrt{N}\gamma r)}}\cosh(\sqrt{N}\gamma r) \\ - \sinh(\sqrt{N}\gamma r)\Bigg)^2. \end{aligned} \tag{32}$$

We first consider the case of zero phase mismatch $\delta = 0$, for which (31) reduces to

$$\begin{aligned} \tilde{\nu}_-' &= [\cosh(\sqrt{N}r) - \sinh(\sqrt{N}r)]^2 \\ &= e^{-2\sqrt{N}r}. \end{aligned} \tag{33}$$

The logarithmic negativity is thus positive and furthermore scales quadratically with the number of modes

$$\mathcal{E}_{\mathcal{N}}(\rho') = 2\sqrt{N}r. \tag{34}$$

Note that the covariance matrix (27) is block-diagonal since (15) entails that $a = \cosh(2\sqrt{N}r)$, $b = \sinh(2\sqrt{N}r)$, and $c = 0$. It is readily recognized that its nontrivial part pertains to two entangled modes with a squeezing parameter $2\sqrt{N}r$ and the remainder to $2N-1$ modes in the vacuum state. This is one instance of the localization of entanglement as introduced in Ref. [3]. The result (34) generalizes the one obtained in Ref. [21] for a single pair of tilted pump ($N = 1$) and shows that the effective squeezing is enhanced by a factor $\sqrt{N}$.

When the phase mismatch takes on some finite values, the logarithmic negativity (31) features the smallest symplectic eigenvalue (30). It is instructive to obtain a more explicit expression for a small phase mismatch by expanding around the case $\delta = 0$,

$$\mathcal{E}_{\mathcal{N}}(\rho') = 2\sqrt{N}r - \frac{\delta^2 r}{\sqrt{N}}\left(1 - \frac{\tanh\sqrt{N}r}{\sqrt{N}r}\right) + O(\delta^4). \tag{35}$$

The correction is of second order in δ and negative. It is a bounded function of N whose magnitude decreases for large N. The positivity of the logarithmic negativity implies that the central mode is entangled with the uniform superposition of the tilted modes. This entanglement localization only slowly decreases when the phase mismath δ increases. This confers some robustness to the entanglement localization process and is somehow in contrast with the multipartite entanglement (18) which seems more sensitive to the phase mismatch. Recalling that the squeezing parameter $r = \sqrt{2}\alpha\lambda\ell$, Eq. (35) also quantifies explicitly the entanglement localization in terms

of the pump amplitude α, the coupling parameter λ, the crystal length ℓ, and provides the scaling with N.

IV. CONCLUSION

We have presented a simple active optical scheme for the generation of spatial multipartite entanglement. It consists in using $2N$ symmetrically tilted plane waves as pump modes in the spatially structured parametric down-conversion process taking place in a nonlinear crystal. We have found the analytical solution of the corresponding model in the rotating wave approximation for arbitrary N and possibly nonzero phase mismatch. We have quantitatively studied the entanglement of the $2N+1$ coupled modes obtained at the output of the crystal. When the phase matching condition is satisfied, the system exhibits multipartite entanglement. It has also been shown to subsist for nonzero values of the phase mismatch.

In addition, our scheme provides a realistic proposal for the experimental realization of entanglement localization. By mixing different spatial modes with beam splitters, we can localize the entanglement distributed at the output of the crystal among all the $2N+1$ spatial modes in only two well-defined modes, formed by the linear combinations of the initial ones. Interestingly, this entanglement localization results in an enhancement of the entanglement by a factor $\sqrt{N}$. Moreover, this process has been shown to be robust with respect to the phase mismatch.

ACKNOWLEDGMENTS

This work was supported by the FET programme COMPAS Grant No. FP7-ICT-212008, the Interuniversity Attraction Poles programme of the Belgian Science Policy Office under Grant No. IAP P6-10 «photonics@be», and by the ICT Impulse Programme of the Brussels-Capital Region under project CRYPTASC.

[1] V. Coffman, J. Kundu, and W. K. Wootters, Phys. Rev. A **61**, 052306 (2000).
[2] G. Adesso, A. Serafini, and F. Illuminati, Phys. Rev. Lett. **93**, 220504 (2004).
[3] A. Serafini, G. Adesso, and F. Illuminati, Phys. Rev. A **71**, 032349 (2005).
[4] G. Adesso, A. Serafini, and F. Illuminati, Phys. Rev. A **73**, 032345 (2006).
[5] G. Adesso and F. Illuminati, in *Quantum Information with Continuous Variables of Atoms and Light,* edited by N. J. Cerf, G. Leuchs, and E. S. Polzik (Imperial College Press, London, 2007), pp. 1–21.
[6] Y. Lian, C. Xie, and K. Peng, New J. Phys. **9**, 314 (2007).
[7] P. van Loock and S. L. Braunstein, Phys. Rev. Lett. **84**, 3482 (2000).
[8] K. Kasai, G. Jiangrui, and C. Fabre, Europhys. Lett. **40**, 25 (1997).
[9] O. Pfister, S. Feng, G. Jennings, R. Pooser, and D. Xie, Phys. Rev. A **70**, 020302(R) (2004).
[10] J. Guo, H. Zou, Z. Zhai, J. Zhang, and J. Gao, Phys. Rev. A **71**, 034305 (2005).
[11] Y. B. Yu, Z. D. Xie, X. Q. Yu, H. X. Li, P. Xu, H. M. Yao, and S. N. Zhu, Phys. Rev. A **74**, 042332 (2006).
[12] A. Ferraro, M. G. A. Paris, M. Bondani, A. Allevi, E. Puddu, and A. Andreoni, J. Opt. Soc. Am. B **21**, 1241 (2004).
[13] M. K. Olsen and A. S. Bradley, Phys. Rev. A **74**, 063809 (2006).
[14] A. V. Rodionov and A. S. Chirkin, JETP Lett. **79**, 253 (2004).
[15] C. H. Monken, P. H. Souto Ribeiro, and S. Pádua, Phys. Rev. A **57**, 3123 (1998).
[16] L. A. Lugiato, A. Gatti, and E. Brambilla, J. Opt. B: Quantum Semiclass. Opt. **4**, S176 (2002).
[17] K. Wagner, J. Janousek, V. Delaubert, H. Zou, C. Harb, N. Treps, J.-F. Morizur, P. K. Lam, and H. A. Bachor, Science **321**, 541 (2008).
[18] L. Lopez, B. Chalopin, A. R. de la Souchère, C. Fabre, A. Maître, and N. Treps, Phys. Rev. A **80**, 043816 (2009).
[19] S. P. Walborn, D. S. Lemelle, M. P. Almeida, and P. H. Souto Ribeiro, Phys. Rev. Lett. **96**, 090501 (2006).
[20] A. S. Coelho, F. A. S. Barbosa, K. N. Cassemiro, A. S. Villar, M. Martinelli, and P. Nussenzveig, Science **326**, 823 (2009).
[21] D. Daems, F. Bernard, N. J. Cerf, and M. I. Kolobov, J. Opt. Soc. Am. B **27**, 447 (2010).
[22] P. van Loock and A. Furusawa, Phys. Rev. A **67**, 052315 (2003).
[23] J. F. Leandro and F. L. Semião, Phys. Rev. A **79**, 052334 (2009).
[24] M. I. Kolobov, Rev. Mod. Phys. **71**, 1539 (1999).
[25] M. Reck, A. Zeilinger, H. J. Bernstein, and P. Bertani, Phys. Rev. Lett. **73**, 58 (1994).
[26] A. Peres, Phys. Rev. Lett. **77**, 1413 (1996).
[27] M. Horodecki, P. Horodecki, and R. Horodecki, Phys. Lett. A **223**, 1 (1996).
[28] R. Simon, Phys. Rev. Lett. **84**, 2726 (2000).
[29] R. F. Werner and M. M. Wolf, Phys. Rev. Lett. **86**, 3658 (2001).